Therapeutic targeting of protein degradation in autoimmunity and cancer

Verbrugge, C.S.E.

2014

document version
Publisher's PDF, also known as Version of record

Multifactorial mechanisms of resistance to the aminopeptidase inhibitor prodrug CHR2863 provoke marked sensitization to the mTOR inhibitor rapamycin

8

Submitted

Sue Ellen Verbrugge,
Marjon Al,
Yehuda. G. Assaraf,
Sarah Kammerer,
Durga M.S.H. Chandrupatla,
Richard Honeywell,
Rene P.J. Musters,
Elisa Giovannetti,
Tom O'Toole,
George L. Scheffer,
David G. Krige,
Tanja D. de Gruijl,
Hans W.M. Niessen,
Willem F. Lems,
Ben A.C. Dijkmans,
Gert J. Ossenkoppele,
Rik. J. Scheper,
Godefridus J. Peters,
Gerrit Jansen.

Departments of Rheumatology, Medical Oncology, Pathology and Cardiac Surgery, ICaR-VU and Hematology, VU University Medical Center, Amsterdam, The Netherlands; Depts. of Physiology and Molecular Cell Biology, VU University, Amsterdam, The Netherlands; The Fred Wyszkowski Cancer Research Laboratory, The Technion-Israel Institute of Technology, Haifa, Israel; Chroma Therapeutics Ltd, Abingdon, United Kingdom

Abstract

Carboxylesterases (CES) play a pivotal role in intracellular metabolic processes of drug detoxification or activation as well as lipid/cholesterol homeostasis. Here we report the molecular basis of acquired resistance to CHR2863, an orally available hydrophobic aminopeptidase inhibitor (AP) prodrug with an esterase-sensitive motif. CHR2863 can enter target cells by diffusion and is retained therein upon CES-mediated conversion to its active hydrophilic metabolite drug CHR6768 to exert amino acid depletion. From CHR2863-sensitive human U937 myeloid leukemia cells, one subline U937/CHR2863(200) with a low level (14-fold) and another, U937/CHR2863(5uM), with a high level (270-fold) of CHR2863 resistance were selected for further characterization. The main features of CHR2863-resistant cells included: (1) a marked down-regulation of CES1 mRNA (3-5 fold) and CES1 protein, mirrored by a 4-7 fold increase in CES2 mRNA, a modest increase in CES2 protein, along with a gain of sensitivity to the CES2-activated prodrug CPT11/irinotecan; (2) loss of CES1 immunoreactivity and colocalization with lipid droplets as observed in parental U937/WT cells by 3D digital imaging fluorescence microscopy; (3) a 40-50% increase in lipid droplets count and intracellular sequestration of CHR2863, associated with a loss of conversion to its active metabolite, and; (4) a progressive activation of pro-survival Akt/mTOR pathway, coinciding with a dramatic gain of sensitivity to the mTOR inhibitor rapamycin in U937/CHR2863(200) cells (54-fold) and U937/CHR2863(5uM) cells (>1,000-fold).

In conclusion, impaired CES1-mediated drug activation, sequestration in lipid droplets and Akt/mTOR activation, contribute to a multifactorial mechanism of resistance to CHR2863, which can be overcome by rapamycin or CES2-activated prodrugs.

Introduction

Aminopeptidases (AP) play an essential role in protein and peptide homeostasis by regulating their modification, maturation, activation and degradation.[1] Small peptides may either be completely hydrolyzed to amino acids for

renewed protein biosynthesis or trimmed for major histocompatibility class I presentation to initiate $CD8^+$ T cell-mediated immune responses.[2] Moreover, plasma membrane-associated APs such as aminopeptidase N (CD13) can serve as cell function mediators, e.g. in signal transduction pathways in immune cells or endothelial cells.[3–5] Consequently, the relevance of APs extends to malignant and (chronic) inflammatory diseases and may thus provide opportunities for therapeutic interventions. [6–9] In this context, bestatin represented the first prototypic AP-inhibitor tested in a clinical setting and displayed immune-modulatory properties through suppression of the production of pro-inflammatory cytokines by activated macrophages as well as anti-proliferative activity in lung cancer and acute myeloid leukemia.[10–12] Building on bestatin as a direct AP inhibitor, also prodrug versions of AP-inhibitors are now being evaluated, of which tosedostat (CHR2797) revealed promising clinical activity against acute myeloid leukemia, multiple myeloma and solid tumors.[13–18] As a hydrophobic prodrug Tosedostat harbors a cyclopentyl ester that requires intracellular cleavage by (carboxyl) esterase activities to yield a hydrophilic acid form that facilitates its intracellular retention. Since carboxylesterases are highly expressed in myelomonocytic leukemia cells, this may underlie Tosedostat's activity towards AML.[19,20] Tosedostat blocks multiple APs, including aminopeptidase N (CD13), leucine aminopeptidase and puromycin-specific aminopeptidase.[13] These inhibitory activities were largely retained upon conversion to its active metabolite, although the latter displayed a potent inhibitory to leukotriene A_4 hydrolase.[13] Upon AP inhibition, Tosedostat provoked an intracellular amino acid depletion and suppressed cell growth as part of an amino acid deprivation response as well as inhibition of mTOR.[13,21] As AP prodrugs with esterase motifs are being evaluated in the clinic, we herein addressed the important question as to whether prolonged exposure to these classes of drug would provoke the onset of drug resistance, and if so, elucidate the molecular basis of resistance. We report that human myelomonocytic U937 cells acquired resistance to CHR2863, an orally available close structural analogue of Tosedostat/CHR2797, via multifactorial mechanisms involving down-regulation of carboxylesterase-1 and its association with lipid droplets, prodrug sequestration and lack of conversion to its active metabolite, and activation of Akt/mTOR as pro-survival modality.

We further show that the latter could be exploited to efficiently overcome CHR2863 drug resistance using mTOR-targeted drugs like rapamycin.

Materials and Methods

Chemicals

The compounds CHR2863; (6S)-[(R)-2-((S)-Hydroxy-hydroxycarbamoyl-methoxy-methyl)-4-methyl-pentanoylamino]-3,3 dimethyl-butyric acid cyclopentyl ester, CHR6768; (6S)-[(R)-2-((S)-Hydroxy-hydroxycarbamoyl-methoxy-methyl)-4-methyl-pentanoylamino]-3,3 dimethyl-butyric acid, CHR5346; (6S)-[(R)-2-((S)-Hydroxy-hydroxycarbamoyl-methyl)-4-methyl-pentanoylamino]-3,3 dimethyl-butanoic acid cyclopentyl ester; non-cleavable ester, CHR2875; (S)-[3-(7-Hydroxycarbamoyl-heptanoylamino)-benzylamino-phenyl acetic acid cyclopentyl ester, and CHR2880 ((S)-[3-(7-Hydroxycarbamoyl-heptanoylamino)-benzylamino-phenyl acetic acid) were synthesized by Chroma Therapeutics UK and dissolved in dimethylsulfoxide as 10 mM stock solutions and stored at -20°C.[13,19]

CPT-11/Irinotecan was from Tocris Biosciences (Ellisville, MO, USA), bortezomib from Millennium Pharmaceuticals (Cambridge MA, USA), MTX from Pharmachemie (Haarlem, The Netherlands), carfilzomib from Onyx Pharmaceuticals (South San Francisco, USA), rapamycin (JS Research Chemicals Trading, Wedel, Germany) and MK571 from Enzo Life Sciences (Antwerp, Belgium). Other drugs, including bestatin, daunorubicin, cytarabine (Ara-C), capecitabine (5'-deoxyfluorouridine), Methyl-b-cyclo-dextrin, loperamide, benzil and Nile Red were purchased from Sigma-Aldrich (St. Louis, MO, USA). Triton-X100 and paraformaldehyde were from Merck (Darmstadt, Germany).

Antibodies

The following antibodies were used: CES1 (polyclonal antibody from Proteintech Group, Chicago, IL, USA, 16912-1-AP, and monoclonal antibody from Lifespan Biosciences, Seattle, WA, USA, LS-C498701, both 1:1000 dilution), CES2 (Santa Cruz Biotechnology, Santa Cruz, CA, USA, Sc-100685, 1:250 dilution, and Life

Span Bio, clone 4F12, LS-B6190, 1:500 dilution), CES3 (1:1000, Protein Europa, 14587-1-AP, 1:1000 dilution) and MRP1 (MRPr1, 1:500), MRP2 (M2 III-6, 1:500), MRP3 (M3 II-21, 1:500), MRP4 (M4 I-10, 1:250), MRP5 (M5 I-10, 1:250), Pgp (JSB1, 1:500), BCRP (BXP53, 1:200) as described before.[22] The following rabbit antibodies were all used from Cell Signalling Technology (Danvers, MA, USA) at a 1:1000 dilution: Total Akt (#9272), phospo-Akt (Ser308) (C31E5E) (#2965), phospho-Akt (Ser473) (#9271), total mTOR (7C10) (#2983), phospho-mTOR (Ser2448) (#2971), phospho-mTOR (Ser2481) (#2974), total S6 kinase (#9205), phospho-S6 kinase (Thr389) (#9205). β-Actin antibody was from Sigma-Aldrich, St. Louis, MO, USA, A2172, 1:10,000). Secondary antibodies included goat anti-mouse or goat anti-rabbit antibodies conjugated to IRDye®800CW (1:10.000, Odyssey; LI-COR, Biosciences, Nebraska, USA); rabbit anti-rat/HRP, rabbit anti-mouse/HRP (1:2000, DAKO, Glostrup, Denmark) or goat anti-rabbit/HRP (1:2000, Santa Cruz Biotechnology, CA, USA) and goat anti-rabbit Alexa 633 (Life Technologies, Paisley, UK).

Cell culture and development of CHR2863 resistance

The human myelomonocytic leukemia cell line U937 (ATCC, Manassas, VA, USA) was grown in RPMI-1640 culture medium (Lonza, Verviers, Belgium) supplemented with 5% fetal calf serum (FCS, PAA Cell Culture Company, Pasching, Austria), 20 mM HEPES, 2 mM L-glutamine, and 100 U/ml penicillin/streptomycin (all from Lonza, Verviers, Belgium). The cell lines were cultured in 25 cm^2 culture flasks (Greiner Bio-One GmbH, Frickenhansen, Germany) in 10 ml medium at an initial density of 3 x 10^5 cells/ml and in a humidified atmosphere at 37°C and 5% CO_2. Cell cultures were refreshed every 3-4 days.
Acquired resistance to CHR2863 was induced by exposing U937/WT cells to a starting concentration of 15 nM CHR2863 (IC_{10}) for one week. Then dosages of CHR2863 were stepwise increased when cells had adapted to drug increments by exhibiting cell growth comparable to control U937/WT cells. Over the course of CHR2863 increments, two sublines of CHR2863 resistant U937 cells were selected for further detailed characterization; (a) one with a relatively low level of acquired resistance (~ 14-fold) isolated after 2.5 months when grown in the presence of 200 nM CHR2863 (further designated as U937/CHR2863(200), and (b) one with a high level of CHR2863 resistance (> 250-fold) isolated after

5-6 months when grown in the presence of 5 μM CHR2863 (further designated as U937/CHR2863(5μM) cells).

Cell growth inhibition assay

Growth inhibition assays on U937/WT cells and CHR2863 resistant sublines were performed essentially as described previously.[23] In short, 0.5 ml cell suspensions were plated in 48-well plates at an initial concentration of 1.25 x 10^5 cells/ml. An untreated control and 7 different drug concentrations (covering 2 log concentrations) were included in each experiment. As vehicle control, maximal concentrations of 0.06% DMSO were included. Cells were grown in a humidified atmosphere at 37°C and 5% CO_2 and after 72 hours drug exposure, cell counts were performed with a hemocytometer and cell viability was checked by trypan blue exclusion.

RNA isolation, cDNA synthesis and qRT-PCR CES1 & CES2, CES1 siRNA

Extraction of total RNA from 1-2 x 10^6 cells was performed with Trizol (Invitrogen, Paisley, UK) according to manufacturers. For cDNA synthesis, the DyNAmo cDNA Synthesis Kit (Thermo Scientific, Waltham, MA, USA) was used as follows: 500 ng RNA were diluted with RNase-free water to a total volume of 7 μl and mixed with 10 μl RT buffer (containing 10 mM $MgCl_2$ and a dNTP mix), 1 μl of random hexamers (300 ng/μl) and 2 μl of M-MuLV RNase H^+ reverse transcriptase. The reverse transcription (RT) PCR was performed under following conditions: 10 minutes at 25°C for primer extension, 30 minutes at 37°C for cDNA synthesis and 5 minutes at 85°C to terminate the reaction (inactivation of M-MuLV). The samples were stored at -20°C until use.

qRT-PCR was performed to determine the expression levels of CES1 and CES2 mRNA. cDNA was diluted 1:10 by adding 180 μl of RNase-free water to the sample volume of 20μl. For a duplicate reaction, 29.5 μl of the TaqMan Universal PCR Master Mix (Applied Biosystems, Foster City, CA, USA), 15.5 μl RNase-free water and 2.5 μl probed primers (TaqMan Gene Expression Assays Hs00275607_m1 for CES1, Hs00187279_m1 for CES2 and Human ACTB Endogenous Control (VIC®-MGB, probe # 4326315E for β-actin, all from Applied Biosystems) were mixed with 12.5 μl of diluted cDNA. 25 ml of each mix were transferred in

duplicate to a 96-well PCR plate. The qRT-PCR was performed with the Applied Biosystems 7500HT sequence detection system apparatus utilizing optimal primer concentrations, i.e., associated with minimum standard deviations between C_T values. A validation experiment was performed to demonstrate that the efficiencies of the target (CES1 and CES2) and reference (β-actin) gene amplifications were approximately equal, using a standard curve method with several dilutions (from 1:10 to 1:10000) of a cDNA sample from untreated control cells.

The results were analyzed using the ΔΔCt method, where Ct values are normalized to the reference gene (β-actin) and shown relative to a control. Relative mRNA expression levels are depicted as $2^{(-\Delta\Delta Ct)}$, i.e. $2^{(-Ct\,target\,-\,Ct\,\beta\text{-}actin\,-\,Ct\,control)}$.

Knockdown of CES1 expression was performed Silencer Select pre-designed siRNA (Applied Biosystems, siRNA ID S2921), sense: CCAUGGAGCUUUGUGAAGAtt, antisense: UCUUCACAAAGCUCCAUGGtt according to manufacturers' procedures. In short, U937/WT cells were resuspended in 20°C serum-free RPMI medium at an initial density of 4 x 10^5 cells/ml. A solution of CES1 siRNA (25 pmol in nuclease-free water) or Stealth RNAi negative control (Invitrogen, Carlsbad, CA, USA) were preincubated with lipofectamine (Invitrogen) for 10 minutes at room temperature and then added to the cells. After 4 hours incubation, 10% FCS was added to each flask and after 24 hours, cells were collected and analyzed for CES1 knockdown efficiency by qRT-PCR as described above.

Western blotting

Cells (3 x 10^6) were harvested in the mid-log phase of growth, washed 3 times with ice-cold PBS after which cell lysates were prepared by resuspending in 150 ul lysis buffer (Cell Signaling Technology, #9803) containing 4% PIC (Protease Inhibitor Cocktail) and 1 mM $NaVO_4$. After centrifugation (13,000 x g for 10 min), protein content in the supernatant fraction was determined with the Bio-Rad Protein Assay (Munich, Germany). Protein aliquots (30 µg) of cell lysates were fractionated on a 4-20% TGX pre-cast SDS PAGE gel (BioRad) and next transferred onto a polyvinylidene difluoride (PVDF) membrane (Millipore, Billerica, MA, USA) suitable for the Odyssey Infrared Imaging System (PerkinElmer, Zaventem, Belgium) for chemoluminescent detection. The membranes were pre-incubated for 1 hour in blocking buffer (Odyssey Blocking Buffer, LI-COR, Biosciences) or

PBST (PBS and 0.05% Tween20, Merck, Darmstadt, Germany) containing 5% non-fat dry milk (Biorad, Munich, Germany). After blocking, the membranes were incubated overnight at 4ºC with specific primary antibodies. β-Actin was used as the control for equal loading. After 3 washing steps with PBS/0.05% Tween20 (Merck, Germany), the membranes were incubated for 1 hour with appropriate secondary antibodies. Detection of antibody binding was obtained using the LI-COR Odyssey scanner (Biosciences) according to the manufacturers' instructions, or incubated for 5 minutes with the ECL Plus detection solution (GE Healthcare, Buckinghamshire, UK) and exposed to an Amersham high performance chemoluminescence film (GE Healthcare, Buckinghamshire, UK). Digital image acquisition and quantification was performed using the Odyssey infrared imaging system software (version 3.0.16, LI-COR Biosciences, Nebraska, USA)

LC-MS/MS analysis of CHR2863 prodrug conversion to its acid metabolite CHR6768

Intracellular conversion of CHR2863 to its acid form and active metabolite CHR6768 was analyzed by incubating 1.5 x 10^6 U937/WT and U937/CHR2863 cells (in the absence of selecting drug) in a 25 cm^2 tissue culture flask in 5 ml RPMI-1640 medium/5% FCS at 37°C in a humidified 5% CO_2 atmosphere. After 24 hours, cells were exposed for 6 hours to 6 μM CHR2863 (unless otherwise indicated). Cells were then centrifuged and 500 ml of supernatant conditioned medium collected and stored at -80°C. Cells were then washed twice with 7.5 ml ice-cold PBS, counted and snap frozen at -80°C for analysis. A similar procedure was followed for assessment of conversion of the HDAC-inhibitor prodrug CHR2875 to CHR2880.[19] Analysis for CHR2863 and CHR2875 and their primary active metabolite were determined by a validated liquid chromatography tandem mass spectrometric assay, essentially as described by Krige et al.[13] Briefly, frozen cell pellets were allowed to warm to room temperature before being re-suspended in minimum quantity of purified water. The subsequent homogenous suspension was diluted with water to achieve 5.0 x 10^6 cells per ml, prior to being snap frozen in liquid nitrogen. Following re-thawing 100 μl of the homogenized cell suspension was extracted with 40 μl of acetonitrile containing 250 μg/ml BB-1090 (internal standard). After 10 minutes ultra-

sonication and centrifugation (2 min, 10 000 g) 50 µl of the supernatant was transferred to 96 well plate for LCMS/MS analysis.

Optimized liquid chromatography was performed on a 4 µm C18 Hyperclone column (Phenomenex, 50 x 2 mm) with gradient elution over 4 minutes at a flow rate of 250 µl/min. Initial conditions consisted of 85% A (aqueous 0.1% formic acid) and 15 % B (0.1% formic acid in acetonitrile), changing to 15% A: 85% B after 1 minute and subsequently holding for a further 3 minutes. Mass spectroscopic detection was performed at optimized conditions as follows; Ion spray voltage - 3800 volt, Capillary temperature 420°C, nebulizer gas - 10 litres per minute, auxiliary gas – 6 litres per minute. Detection parameters for each mass were optimized with mobile phase B for CHR2863 (421.1 / 260.1), CHR6768 (353.160 / 260.1) CHR2875 (496.0 / 382.2), CHR2880 (428.0 / 382.2) and BB-1090 (366.2 / 119.7). Data quantification was performed with Analyst (AB sciex B.V) version 5.2 in combination with Dionex Mass Link chromatography software version 2.10.

IMAGE STREAM ANALYSIS FOR LIPID DROPLET COUNTS

Cells (2 x 10^6) in the mid-log phase of growth were harvested and washed 3 times with PBS/0.1% BSA and resuspended in 1 ml PBS/0.1% BSA. Cells were then incubated in the dark for 4 min at 25°C with Nile Red (0.1 µg/ml final concentration from stock solution of 1 mg/ml in 10% acetone). Cells were then washed 3 times protected from light with ice-cold PBS/0.1% BSA and processed by ImageStream ISX analysis (Amnis, Seattle, WA, USA), an instrument that combines microscopy and flow cytometry in one platform. By imaging cells in flow, the system – on a per cell basis – allows the measurement of brightness, size and location of fluorescently labeled subcellular components and compilation of this data into the population statistics of conventional FACS analysis. The analysis software (Amnis, Seattle) utilizes two tool sets; “masks” giving location to an object in an image and “features” enabling measurement of the physical properties of the objects defined by the mask. Thus, Nile Red labeled lipid droplets in a cell were masked as objects with a user defined pixel radius and brightness. The spot count feature then counted the objects that met these criteria. The data is displayed as the percentage of cells in a given sample with a specified number of spots from a minimum of 10,000 cells analyzed.

3D DIGITAL IMAGING FLUORESCENCE MICROSCOPY

Cytospins were prepared of U937/WT, U937/CHR2863(200nM) and U937/CHR2863(5μM) cells grown for 2 days in absence of selecting drugs. Cells were then fixed with 4% paraformaldehyde in PBS for 10 min at room temperature. After washing the slides with PBS, cells were permeabilized with PBS/0.1% Triton-X100 for 10 min at 4ºC. After washing with PBS, the cells were blocked in 10% FCS for 30min at room temperature. Next, cells were washed three times in 100 μl PBS and then incubated with primary CES1 polyclonal antibody (1:400 diluted in PBS/0.1%BSA) and incubated for 1 hour at room temperature. Cells were then washed three times with PBS and incubated with secondary antibody (goat anti-rabbit Alexa 633, 1:300 diluted in PBS/0.1%BSA) for 45 min at room temperature. After three times washing, cells were stained with Nile Red (1:2500 dilutions from stock solution of 1 mg/ml in 10% acetone in PBS) for 5 min. After washing 3 times with PBS, cells were air dried in a flow chamber for 1min followed by DAPI staining. The cytospin preparation was the covered by a cover slip, fixed with nail polish, and prepared to microscopical analysis. To this end, fixed cells were examined with a Zeiss Axiovert 200M Marianas™ inverted microscope, equipped with a motorized stage (stepper-motor z-axis increments: 0.1 μm), and a turret of four epifluorescence cubes (FITC, Cy-5, Cy-3, AMCA as well as a DIC bright field cube). A cooled CCD camera (Cooke Sensicam SVGA [Cooke Co., Tonawanda, NY], 1,280 × 1,024 pixels) recorded images with true 16-bit capability. The camera is linear over its full dynamic range (up to intensities of over 4,000) while dark/background currents (estimated by the intensity outside the cells) is typically <100. Exposures, objective, montage, and pixel binning were automatically recorded with each image stored in memory (Dell Dimension workstation: Quad-core processor, 16GB RAM). The microscope, camera, and data processing were controlled by SlideBook™ software (SlideBook™ version 5.5.2.0 [Intelligent Imaging Innovations, Denver, CO]). All microscopy was performed with a custom 40X or 63X oil-immersion lens (Zeiss). The motorized filter cubes allowed acquisition of one composite image (on all four different fluorescent wavelengths) within 2 s. The data acquisition protocol included optical planes to obtain 3-D definition. Moreover, the software used is fully equipped to acquire, process (several deconvolution

modes), and display true 3-D data and was used throughout the experiments.

Electron microscopy

Cells in mid-log phase of growth were fixed using an overnight incubation in 2% (vol/vol) glutaraldehyde in phosphate buffer for 30-minutes and 1.5% (wt/vol) osmium tetroxide for 10 minutes, dehydrated with acetone, and embedded in Epon812. Ultrathin sections (60-70 nm) were collected on 300-mesh Formavar-coated nickel grids. The sections were counterstained with 2% uranyl acetate and lead citrate and were examined in a Jeol 1200EX electron microscope. Photographs were finally printed using a Leitz Focomat IIc.

Cholesterol assay

Intracellular levels of cholesterol and cholesterylesters were determined by the Amplex Red fluorometric assay (Molecular Probes, Eugene, OR, USA) according to the manufacturers' procedure and described by Li et al.[24] Briefly, 1 x 10^6 cells were harvested at day 1, 2 and 3 after plating of regular cell cultures of U937/WT cells, U937/CHR2863(200) and U937/CHR2863(5uM) cells at their selective concentrations of CHR2863 in the medium. Cells were washed 3 times with ice-cold PBS and aliquots of 2 x 10^5 cells were centrifuged in Eppendorf tubes and cell pellets were stored at -20^{o}C until analysis. Levels of total cholesterol (free-cholesterol and cholesterylesters) were expressed as ng/10^6 cells. As a control, cholesterol levels were analyzed in U937/WT cells incubated with 1 mM of the cholesterol-depleting agent methyl-β-cyclo-dextrin (MβCD).

Statistics

For comparison between groups a two-sided paired Student's t tests was used. Differences were considered to be significant at $p < 0.05$.

Results

Development of CHR2863 resistance and cross-resistance profile.

CHR2863, a structural analogue of Tosedostat (CHR2797) with a methoxy-group in the hydroxycarbamoyl moiety (Fig 1A) was administered to human

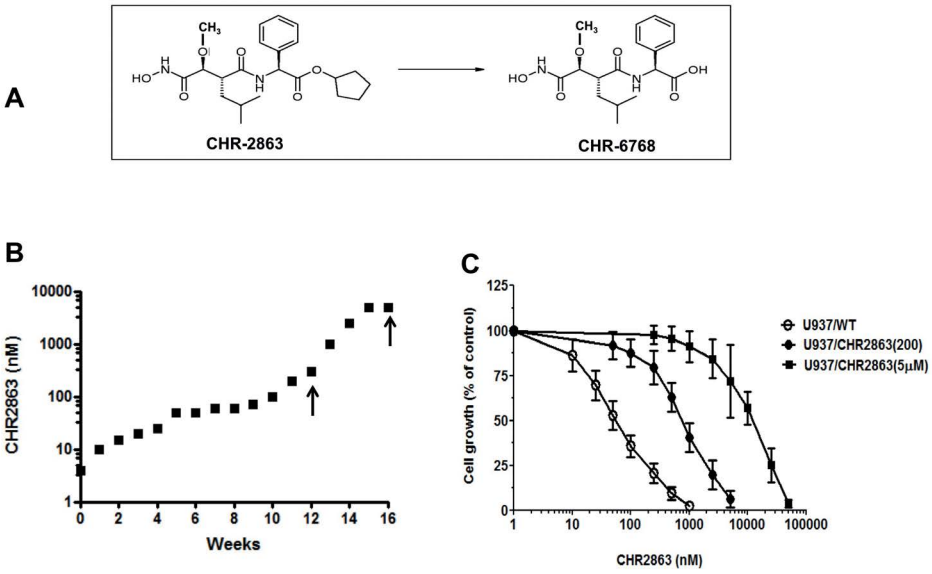

Figure 1. (A) Chemical structure of the aminopetidase inhibitor prodrug CHR2863 with an esterase motif and its acid metabolite CHR6768. (B) Time line for acquisition of resistance to CHR2863 in U937 cells. *Two isolates (indicated by arrows) were selected for further characterization; U937 cells grown in the presence of 200 nM CHR2863 (U937/CHR2863(200) cells) and U937 cells grown in the presence of 5 μM CHR2863 (U937/CHR2863(5μM) cells). (C) Dose response curve of for growth inhibition by CHR2863 for U937/WT, U937/CHR2863(200), and U937/CHR2863(5μM) cells. Results depicted are the mean ± SD of 7-10 separate experiments.*

myelomonocytic U937 cells in stepwise increasing doses over a period of 4-6 months. During this multiple step selection U937 acquired resistance to CHR2863 (Fig. 1B) and two selectants were isolated for further characterization; one with a low level resistance grown at a concentration of 200 nM CHR2863 (U937/CHR2863(200)) and another with a high level resistance grown at a concentration of 5μM CHR2863 (U937/CHR2863(5μM)). Dose response curves for CHR2863-induced growth inhibition for U937/WT and the two selectants are shown in Figure 1C. Resistance factors were calculated to be 13.7-fold for U937/CHR2863(200) cells and as high as 270-fold for U937/CHR2863(5μM) cells (Table 1). Cross resistance profiling for other selected (pro)drugs (Table 1) showed lack of cross-resistance to the direct AP-inhibitor bestatin and CHR5346

Table 1. Growth inhibitory effects of aminopeptidase inhibitor prodrug CHR2863 and other (pro) drugs for parental U937 myelomonocytic cells (U937/WT) and sublines of U937 cells with acquired resistance to CHR2863

	IC_{50}		
Drug	**U937/WT**	**U937/CHR2863(200nM)**	**U937/CHR2863(5µM)**
CHR2863 (nM)	**52 ± 16**	**713 ± 212*** (13.7)**	**14,047 ± 5,521*** (270)**
Bestatin (µM)	**149 ± 21**	**151 ± 45 (1.0)**	**177 ± 12 (1.2)**
CHR5346 (µM)	**8.4 ± 1.4**	**9.3 ± 1.1 (1.1)**	**13.7 ± 4.2 (1.6)**
CHR2875 (nM)	**152 ± 30**	**84 ± 10*** (0.55)**	**158 ± 33 (1.0)**
CPT-11/Irinotecan (µM)	**1.37± 0.29**	**0.60 ± 0.18** (0.44)**	**0.45 ± 0.10** (0.33)**
Capecitabine (Xeloda) (mM)	**1.5 ± 0.3**	**3.3 ± 0.3** (2.2)**	**3.4 ± 0.3** (2.3)**
Ara-C (nM)	**49 ± 14**	**59 ± 24 (1.2)**	**23 ± 10** (0.47)**
Daunorubicin (nM)	**16 ± 2**	**15 ± 1 (1.0)**	**15 ± 2 (1.0)**
Bortezomib (nM)	**3.5 ± 0.5**	**5.8 ± 1.8* (1.7)**	**4.1 ± 0.8 (1.2)**
Carfilzomib (nM)	**4.9 ± 1.3**	**7.3 ±1.2* (1.5)**	**6.9 ± 1.3 (1.4)**

*Cell growth inhibition was determined after 72 hrs drug exposure and results depicted are the mean IC_{50} values of 4-7 independent experiments ± S.D. IC_{50} is defined as drug concentration resulting in 50% growth inhibition compared to control. Values between brackets represent Resistance Factor, defined as the ratio of IC50 value of U937/CHR2863-resistant cells over IC_{50} of parental U937/WT cells. Statistics: *p<0.05, **p<0.01, ***p<0.001 (resistant cells vs wild type cells).*

(a non-cleavable analogue of CHR2797), suggesting that alterations in AP-levels do not contribute to CHR2863 resistance. CHR2863-resistant cells also retained sensitivity to CHR2875, an HDAC-inhibitor prodrug.[19] Interestingly, CHR2863-resistant cells displayed acquired collateral sensitivity (2-3 fold) to the topoisomerase inhibitor prodrug CPT-11/irinotecan, but were 2-fold

less sensitive to the 5-fluorouracil prodrug Capecitabine/Xeloda. CHR2863-resistant cells retained sensitivity to cytarabine and daunorubicin, two drugs which are usually combined with Tosedostat/CHR2797 in AML therapy.[14] Finally, growth inhibitory effects of two proteasome inhibitors bortezomib (Velcade) and carfilzomib, functioning upstream of APs in protein degradation pathways, were unaltered in CHR2863-resistant cells.[23] Examination of the stability of the drug resistance phenotype revealed that in the absence of selecting drug, U937/CHR2863(200) cells rapidly lost (within 1 month) their CHR2863 resistance. In contrast, U937/CHR2863(5μM) cells retained their drug resistance in the absence of CHR2863 for > 3 months, thereby suggesting a genetically stable resistance phenotype (results not shown). As an initial approach to unravel the molecular basis underlying CHR2863 resistance, we explored whether drug extrusion via multidrug resistance (MDR)-related drug efflux transporters could be involved as they can extrude a broad spectrum of hydrophobic drugs (e.g. CHR2863) or hydrophilic drugs (e.g. CHR6768, the acid form of CHR2863).[25] Western blot analysis of a series of drug efflux transporters revealed either no detectable expression of these MDR efflux transporters (P-glycoprotein, MRP2 and MRP3) or no differential expression (MRP1, MRP5 and BCRP) in U937/WT and a series of CHR2863-resistant U937 cells (Suppl Fig. S1). Of notice, expression of MRP4 was gradually increased in U937 cells with increasing levels of CHR2863 resistance. Elevated levels of MRP4 were, however, not directly accountable for conferring CHR2863 resistance as co-incubation with an established inhibitor of MRP4 (i.e. MK571) had no reversal effect on CHR2863 resistance (results not shown). Together, these results and cross-resistance profiling point to a non-classical mechanism of CHR2863 resistance.

Intracellular sequestration CHR2863 and lack of conversion of CHR2863 to active metabolite in U937/CHR2863(5μM) cells.

Since conversion of CHR2863 to the hydrophilic acid metabolite CHR6768 contributes to its pharmacological activity, we examined this capacity in U937/WT and U937/CHR2863 cells. U937/WT displayed proficient and linear (not shown) conversion of CHR2863 into CH6768 (338 ± 63 ng/10^6 cells) over a 6 hr exposure to 6 μM of CHR2863 (Figure 2A). Under these conditions,

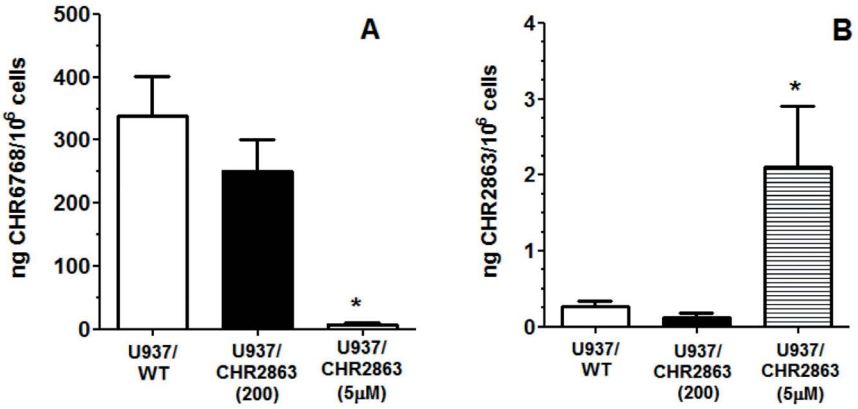

Figure 2. (A) Conversion of CHR2863 to CHR6768 and (B) retention of CHR2863 in U937/WT, U937/CHR2863(200), and U937/CHR2863(5μM) cells *after 6 hr exposure to 6 μM CHR2863. Results are expressed as ng/10^6 cells and represent the mean ± SE of 7-9 separate experiments. (*): p<0.001*

U937/CHR2863(200) cells displayed a 24% reduced conversion to CHR6768 (251 ± 47 ng drug/10^6 cells) as compared to U937/WT cells. Strikingly, however, conversion of CHR2863 to CHR6768 in U937/CHR2863(5μM) cells was almost completely abolished to 7.3 ± 2.2 ng drug/10^6 cells, thereby losing 98% of parental U937/WT enzymatic conversion. Additionally, beyond conversion to the active metabolites, we also analyzed the levels of CHR2863 prodrug retained in these 3 cell lines (Fig. 2B). In U937/WT and U937/CHR2863(200) cells, absolute intracellular levels of CHR2863 were 3 orders of magnitude lower than those of CHR6768; 0.27 ± 0.07 ng CHR2863 /10^6 cells and 0.12 ± 0.05 ng CHR2863/10^6 cells), respectively. Remarkably, U937/CHR2863(5μM) cells retained significantly higher levels (8-17 fold) of prodrug (2.0 ± 0.8 ng CHR2863/10^6 cells) compared to U937/WT and U937/CHR2863(200) cells, thus suggesting sequestration of the prodrug in these cells and escape from conversion to CHR6768. As a comparison we determined the cellular levels of the HDAC prodrug inhibitor CHR2875 and its active metabolite CHR2880 after 6 hours of exposure to 6 μM CHR2875. Of note, absolute levels of CHR2880 conversion were approximately 100-fold lower than for CHR6768, but no significant differences in levels of CHR2875 and CHR2880, respectively, were observed for U937/WT (0.43 ± 0.18 and 3.6 ± 0.2 ng/10^6 cells), U937/CHR2863(200) cells (0.55 ± 0.15 and 3.0 ± 1.6

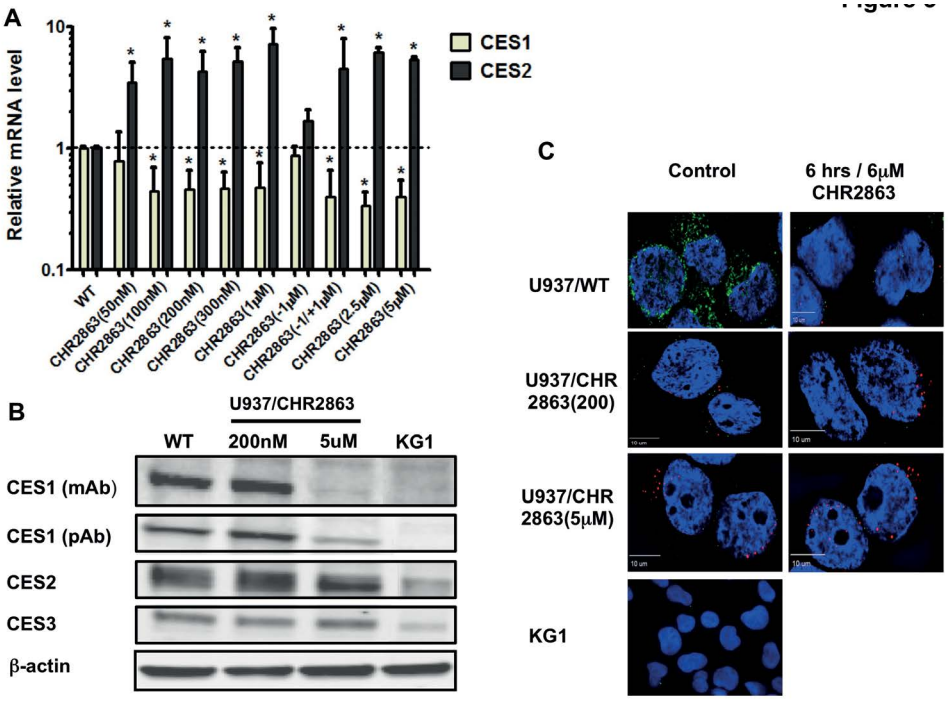

Figure 3. (A) mRNA expression of CES1 and CES2 in multiple isolates of CHR2863-resistant U937 cells, including U937/WT, U937/CHR2863(200), and U937/ CHR2863(5μM) cells. *U937/CHR2863(w/o 1 μM) without CHR2863 for 2 weeks and U937/ CHR2863 (w/o 1μM/+1μM) rechallenged with 1 μM CHR2863 for 2 weeks. Mean (± SD) of 3-4 experiments performed in triplicate). (*): p< 0.05. (B) Western blots of CES1 (by two different antibodies), CES2 and CES3 protein expression in U937/WT, U937/CHR2863(200), and U937/ CHR2863(5μM) cells. KG1 cells served as negative control for CES1 expression [19]. (C) Live cell 3D digital imaging microscopy of CES1 expression in U937/WT, U937/CHR2863(200), U937/ CHR2863(5μM) cells and KG1 cells (as CES1-negative control). Left row represents control conditions, right row represent images after pulse exposure to CHR2863 (6 hr, 6 μM CHR2863).*

ng/10^6 cells) and U937/CHR2863(5μM) cells (0.66 ± 0.05 and 4.3 ± 2.5 ng/10^6 cells), being consistent with a comparable drug sensitivity profile between the parent and resistant sublines shown in Table 1.

These results indicate that at least for U937/CHR2863(5μM) cells, CHR2863 resistance is associated with intracellular drug sequestration along with a markedly impaired conversion to its acid metabolite CHR6768.

Down-regulation of CES1 and upregulation of CES2 in U937/CHR2863 cells.

Since carboxylesterases have an established and prominent role as drug metabolizing enzyme,[19,26–28] we examined whether or not expression of two of its family members known to be expressed in myelomonocytic cells;[20] carboxylesterase 1 (CES1) and carboxylesterase 2 (CES2), were involved in CHR2863 conversion and drug resistance. Analysis of CES1 and CES2 mRNA levels in a range of different U937/CHR2863 cells showed a remarkable down-regulation of CES1 (3-5 fold), being mirrored by an up-regulation of CES2 mRNA (Fig. 3A). Interestingly, when U937/CHR2863(1μM) cells were grown in drug-free medium for 2 weeks, this normalized CES1 and CES2 mRNA to U937/WT levels, but a rechallenge with 1 μM CHR2863 reinforced down-regulation of CES1 and up-regulation of CES2 mRNA (Fig. 3A). To understand whether these dynamics were resistance-induced or could also be noted after pulse exposure (0-6 hrs) to CHR2863, U937/WT cells were exposed to either 50 nM CHR2863 (IC_{50} concentration) or 6 μM CHR2863 (used for metabolite conversion experiments). Both conditions induced CES1 mRNA down-regulation (up to 3-fold) and a comparable up-regulation of CES2 mRNA (Suppl Fig. 2A/B). Since U937/CHR2863(200nM) and U937/CHR2863(5μM) cells were already down-regulated in CES1 and up-regulated in CES2 mRNA expression, pulse exposure to 6 μM CHR2863 only modestly increased this differential or had no additional effect, respectively (Suppl. Fig. 2C/D). We next examined whether differences in CES1 and CES2 mRNA were also reflected at the protein level. CES1 protein levels were not significantly altered in U937/CHR2863(200nM) compared to U937/WT cells, but U937/CHR2863(5μM) cells displayed a markedly down-regulated CES1 expression (Fig. 3B). Rather, CES2 protein expression was modestly increased in both CHR2863-resistant cells compared to U937/WT cells, whereas expression of another CES homologue, CES3, was unaltered (Fig. 3B). The data for CES1 protein expression were further corroborated by live cell 3D digital imaging microscopy studies revealing markedly decreased expression of CES1 in U937/CHR2863(200) cells and a most profound decrease in CES1 expression in U937/CHR2863(5μM) cells, comparable to those in CES1-negative KG1 cellsv(Fig. 3C).[19] Moreover, 3D digital live cell imaging microscopy also showed

a rapid decrease in CES1 immunoreactivity in parental U937/WT cells after 6hr pulse exposure to 6 μM CHR2863 (Fig. 3C). Since this pulse exposure had no effect on CES1 protein levels analyzed by Western blotting (results not shown), this points to CHR2863-induced conformational alterations in CES1 which impair antibody binding to the enzyme in its native state. CES1 knockdown by CES1 siRNA was performed in U937/WT cells which resulted in 85% reduction of CES1 mRNA expression and a 35% reduced conversion of CHR2863 to its active metabolite in U937/WT controls. This reduction, however, had no significant impact on growth inhibitory effects of CHR2863 (not shown), suggesting that knock down of CES1 did not reach a critical level to fully impair CHR2863 conversion and thereby confer resistance.

Beyond a pharmacologic function of CES1 in drug metabolism, the enzyme is also physiologically implicated in cholesterol homeostasis by regulating the hydrolysis of cholesterylesters to free cholesterol.[29,30] To explore whether the marked down regulation of CES1 in U937/CHR2863(5μM) cells had an impact on cellular cholesterylester and free cholesterol content, these parameters were followed during 1-3 day cell growth (Suppl. Fig. S3). After one day in culture, U937/CHR2863(5μM) cells had significantly higher levels of cholesterylesters as compared to U937/WT cells. Upon prolonged cell growth, cholesterylester levels in U937/CHR2863(5μM) were normalized to those of U937/WT and U937/CHR2863(200) cells.
Together, these studies indicate that CHR2863 induces differential response in CES1 and CES2 expression which, upon prolonged exposure, may contribute to acquisition of CHR2863 resistance and also impact cellular cholesterol homeostasis.

Increased number of lipid droplets in U937/CHR2863 cells.

Several studies have pointed out that the catalytic activity of CES1 is enhanced upon hydrophobic interactions with lipid droplets, cell organelles involved, among others, in neutral lipid (triglyceride and sterolester) storage.[29,31,32] Lipid droplets have also been reported in U937 cells and recognized for a role in cancer and inflammatory processes.[33,34] Given this hydrophobic compartment's association with CES1, lipid droplets may deserve consideration as a possible

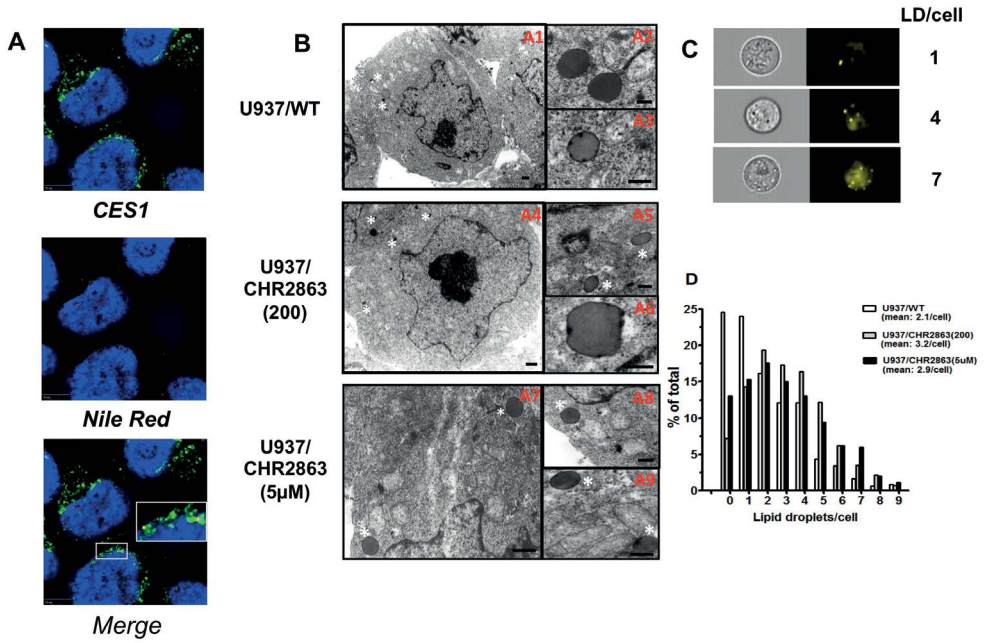

Figure 4. Identification of lipid droplets in U937/WT and CHR2863-resistant cells and CES1-lipid droplet co-localization. *(A) Nile Red staining of lipid droplets and CES1 immunofluorescence detection by 3D digital imaging fluorescence microscopy. Inset depicts colocalization of CES1 with lipid droplets. (B) Transmission electron microscopy identification of lipid droplets (magnification; 4,000-60,000 fold). Bar = 1000 nm (Figure A1, A4, A7), bar = 500 nm (Figure A2, A3, A5, A6, A8, A9). (C) Lipid droplets staining in U937/WT cells with Nile Red and representative examples of image stream analysis sorting cells with 1,4 or 7 lipid droplets per cell, (D) Quantification of the distribution of lipid droplets in U937/WT, U937/CHR2863(200), and U937/CHR2863(5μM) cells by Nile Red staining and image stream analysis allowing assessment of numbers of lipid droplets per individual cell (as in (C)). Mean of two separate experiments performed in duplicate. All experiments included 0.06% DMSO solvent controls.*

site of sequestration of non-metabolized hydrophobic CHR2863 as in U937/CHR2863(5μM) cells (Fig. 2B). Staining of intracellular lipids within lipid bodies by Nile Red and visualization by 3D digital imaging fluorescence microscopy is shown in Fig. 4A, demonstrating variability in numbers and sizes of lipid droplets in U937/WT cells. Additionally, we examined whether CES1 co-localized with lipid droplets, which proved to be the case (Fig. 4A, merged figure and inset). The presence of lipid droplets in U937/WT and CHR2863-resistant cells was further confirmed by transmission electron microscopy (Fig. 4B), which also indicated close physical contact of lipid droplets with mitochondria (Fig. 4B, subsection

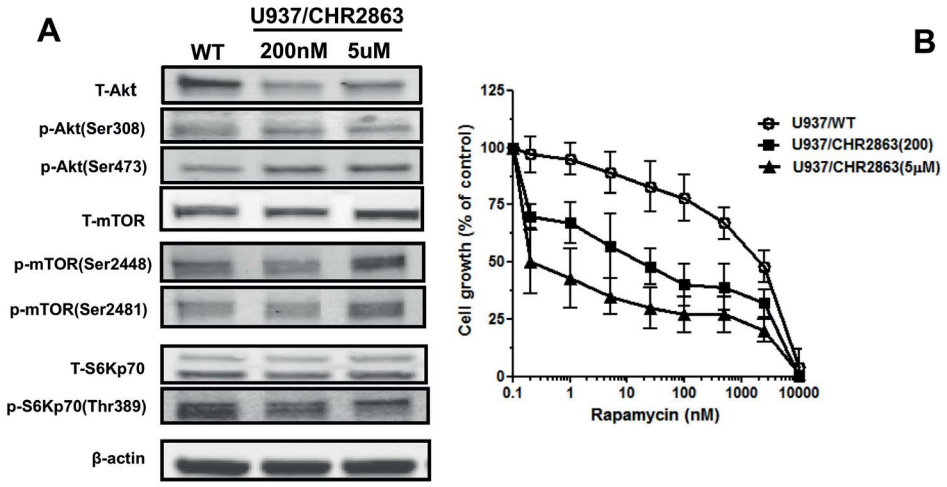

Figure 5. (A) Expression levels of total and phosphorylated mTOR, Akt and S6K in U937/WT, U937/CHR2863(200) and U937/CHR2863(5μM) cells. (B) Inhibition of cell growth by rapamcyin of U937/WT, U937/CHR2863(200) and U937/CHR2863(5μM) cells. *Cell growth inhibition was assessed after 72 hrs drug exposure. Results represent the mean ± SD of 5-7 separate experiments.*

A8 and A9). To quantify lipid droplets in U937/WT, U937/CHR2863(200) and U937/CHR2863(5μM) cells, live stream imaging analysis was performed on Nile Red-stained cells with subsequent sorting of cells based on lipid droplet numbers per cell (Fig. 4C). A representative distribution profile is depicted in Fig 4D, indicating that mean lipid droplet counts in U937/WT cells (2.1/cell) increased by 40% - 50% in U937/CHR2863(200) (3.2/cell) and U937/CHR2863(5μM) cells (2.9/cell). These studies indicate that CHR2863 resistance is associated with increased lipid droplets content in CHR2863 resistant cells.

Activation of Akt/mTOR pathway in U937/CHR2863 cells and marked gain in sensitivity to rapamycin.

Previous studies by Krige et al showed that the AP inhibitors induce an acute response of an intracellular amino acid deprivation leading to reduced

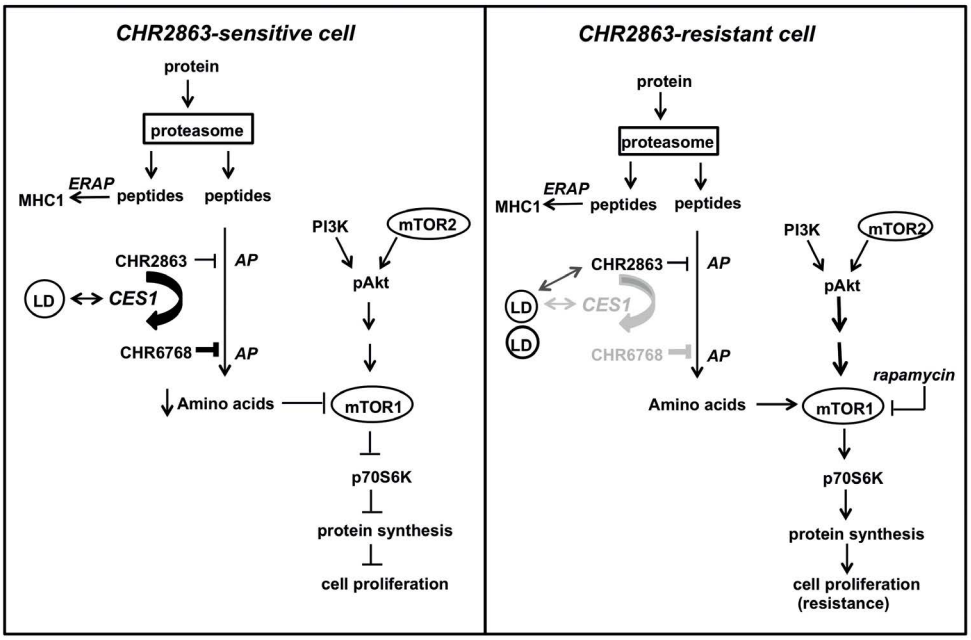

Figure 6. Composite model depicting mechanism of action of CHR2863 sensitivity in U937 cells (left) and mechanism of acquired resistance to CHR2863 in U937/CHR2863(5μM) cells (right). *Parts of the (poly)peptides produced by proteasome-mediated protein degradation are processed for MHC class I presentation involving ERAP (ER-associated aminopeptidase). It is unknown whether CHR2863 or CHR6768 exert inhibitory effects on ERAP. Most polypeptides will be subject to full degradation to amino acids, involving aminopeptidase (AP) action, for renewed protein synthesis. Due to its hydrophobic nature, the cyclopentyl-ester conjugated compound CHR2863 can freely diffuse into cells and has potential to inhibit several APs [13]. The AP-inhibitory potency, however, is significantly improved upon conversion of CHR2863 to its acid metabolite CHR6768 which is accumulated and retained in cells. A likely candidate for CHR2863 conversion includes carboxylesterase 1 (CES1), which has a physiologic function in regulating cholesterol homeostasis, in particular in lipid droplet (LD) cell organelles. Conceivably, CES1 associated with LDs may provide a microenvironment that promotes CHR2863 conversion. CHR6768-induced inhibition of multiple APs will provoke an amino acid depletion which is sensed by mTOR leading to suppression of protein synthesis and inhibition of cell growth. In CHR2863-resistant cells, at least two adaptations took place. One involves a marked down-regulation of CES1 which may convey two effects; (a) rather than conversion, CHR2863 is sequestered in LD, and (b) loss of CHR6768-induced AP inhibition relieves part of the amino acid deprivation pressure, which could contribute to reactivation of mTOR activity. Second, mTOR reactivation may also be initiated separate from CES1 down-regulation (as in U937/CHR2863(200) cells) to promote protein synthesis and cell growth consistent with a resistant phenotype. Activation of mTOR in CHR2863-resistant cells is a targetable entity for its inhibitor rapamycin.*

activity of mTOR as master facilitator of protein synthesis.[13,35] We explored how CHR2863-resistant U937 cells overcame these initial responses by examining the phosphorylation status of mTOR and Akt as indicators of a pro-survival signal. Earlier experiments (not shown) demonstrated that CHR2863-resistant cells had similar levels of [^{14}C]-arginine transport capacity as U937/WT cells and also did not show evidence (based on lack of LC3B cleavage) for autophagy induction as compensatory mechanism. Western blot analysis (Fig. 5A) revealed increased ratios of phosphorylated Akt (Ser473) and phosphorylated mTOR over total Akt and mTOR in resistant cells compared to parental cells, pointing to activation of the Akt/mTOR pathway in CHR2863-resistant cells. A role for mTOR activation in CHR2863-resistant cells was confirmed by a dramatic gain in sensitivity to rapamycin (Fig. 5B); whereas U937/WT cells were relatively insensitive to growth inhibition by rapamycin (IC_{50}: 2260 ± 960 nM), U937/CHR2863(200) cells displayed 54-fold increased sensitivity to rapamycin (IC_{50}: 42 ± 38 nM). Strikingly, rapamycin sensitivity was further enhanced in U937/CHR2863(5μM) cells (IC_{50}: 0.56 ± 0.41 nM), representing > 1,000-fold gain of sensitivity compared to U937/WT cells. These studies indicate that activation of Akt/mTOR can overcome amino acid deprivation effects conveyed by AP-inhibitor drugs as CHR2863. A composite model that accommodates all altered parameters contributing to the molecular basis of resistance to CHR2863 is presented and discussed in Figure 6.

Discussion

Resistance modalities often disclose the Achilles heel of mechanism(s) of action of therapeutic drugs.[36–38] The current study constitutes the first report aimed at unraveling the molecular basis of resistance to CHR2863, an aminopeptidase inhibitor prodrug that structurally mimics the aminopeptidase inhibitor Tostedostat, which shows promising activities in acute myeloid leukemia treatment.[14] CHR2863 is a hydrophobic prodrug with an esterase motif rationally designed to be membrane permeable and activated intracellularly via an esterase-dependent activity that converts it to the active hydrophilic drug CHR6768 that targets multiple aminopeptidases. Here, we demonstrated that acquired

resistance to CHR2863 is a multifactorial mechanism including down-regulation of CES1 expression, impaired prodrug conversion and intracellular sequestration presumably in lipid droplets, as well as activation of mTOR survival pathway.

The role of CES1 in CHR2863 resistance was most evident in U937/CHR2863 (5μM) cells where both a marked down-regulation of CES1 mRNA and CES1 protein were associated with impaired prodrug conversion and a high level of CHR2863 resistance. However, for low level CHR2863 resistant U937/CHR2863(200) cells, down-regulation of CES1 mRNA was not accompanied by similarly reduced CES1 protein levels, albeit a ~ 30% reduction in conversion of CHR2863 to CHR6768 compared to U937/WT cells. This suggests that additional factors contribute to regulation of CES1 protein and catalytic activity at low resistance levels versus highly resistant cells. In this respect, it should be taken into account that within a window of selective concentrations of 200 nM to 5μM, even CHR2863 as a prodrug, in analogy with CHR2797, would impose increasing inhibitory effects on multiple APs, thus calling for additional counter-measures to neutralize these deleterious effects. In macrophages, redistribution of CES1 from the cytoplasm to lipid droplets has been reported in response to lipid loading.[13,39] It is noteworthy that in response to down-regulation of CES1, CES2 was upregulated, probably as a compensatory mechanism. Since upregulation of CES2 had no pharmacologic impact on CHR2863 conversion in U937/CHR2863(5μM) cells, this would imply that CHR2863 is a poor substrate for CES2 and cannot facilitate sufficient conversion to CHR2863 to compensate for CES1 down-regulation. Rather than displaying pharmacological functions, CES2 upregulation may be a physiologic compensatory mechanism preserving some essential cellular functions, in particular in relation to cholesterol homeostasis (i.e. hydrolysis of cholesteryl esters to free cholesterol). Studies by Zhao et al showed that stable over expression of CES1 in human macrophage THP1 cells promoted the extrusion of free cholesterol.[40] Conversely, pharmacologic inhibition of CES1 induced cholesteryl ester retention, whereas shRNA CES1 knockdown in THP1 cells was accompanied by compensatory CES3 upregulation to sustain cholesteryl ester hydrolytic activity.[30,41] Moreover, the same study demonstrated that CES3 transfection decreased the numbers of lipid droplets in THP1 cells. Our data (including Suppl. Fig. S3) are consistent with these observations, except

that in U937/CHR2863 cells CES2 rather than CES3 upregulation may serve as compensatory mechanism. Lastly, EM studies indicating that in CHR2863-resistant cells lipid droplets had physical contacts with mitochondria (Fig. 4B) implying that lipolytic activity within lipid droplets and the release of free fatty acid for b-oxidation in mitochondria holds relevance for energy transfer.[42]

Although direct evidence for sequestration of CHR2863 in subcellular compartments organelles such as lipid droplets would be realistically limited by subcellular fractionation techniques that would retain low quantities of CHR2863 per cell (Fig. 2B), several lines of indirect evidence point to possible role of lipid droplets in the CHR2863 resistance phenotype. Conceivably, CES1 surrounding lipid droplets would provide a more optimal microenvironment for interaction and hydrolysis of a hydrophobic prodrug as CHR2863 than the cytoplasm.[29] Down-regulation of CES1 expression and impaired hydrolysis of CHR2863 would then drive accumulation and sequestration in lipid droplets. In analogy, CHR2863 induced swelling of malaria digestive vacuoles, which are known to harbor lipid droplets.[43–45] Apart from their established role in cholesterol ester storage, lipid droplets have also been recognized as sites of arachidonic acid metabolism leading to the production of leukotrienes and prostaglandins, both mediating inflammatory processes.[33,46] In this regard, it is worthwhile to note that active metabolite of tosedostat displayed potent inhibitory effect on leukotriene A_4 hydrolase activity (IC_{50}: >10,000 nM vs 8 nM, respectively). Indications that the development of CHR2863-resistance was accompanied by alterations in arachidonic acid metabolism could be consistent with observations that U937/CHR2863 cells upregulated the expression of the MDR efflux transporter MRP4 (Suppl. Fig S1), which function has been reported in intracellular vesicles of U937 cells as facilitator of leukotreine B_4, leukotriene C_4 as well as prostaglandin E2 extrusion.[46–48] These considerations come on top of other functions of lipid droplets unrelated to lipid metabolism, including protein trafficking, temporary sequestration of proteins and handling proteins prone for destruction, the latter of which may be of relevance in CHR2863 targeting the proteasome/ aminopeptidase pathway of protein degradation.[32,49–51] In these functions lipid droplets act in a dynamic fashion by organizing transient association with other cellular organelles as

endoplasmic reticulum, mitochondria, endosomes as well as cytoskeleton.

Studies by Krige et al showed that although CHR2797 (Tosedostat) prodrug conversion is a critical step in exerting its pharmacological effect, equally important is whether or not target cells had the capacity to overcome the induction of an amino acid response and consequent suppression of mTOR activity.[13,52] In other words, cells with efficient prodrug conversion but a proficient amino acid deprivation response displayed reduced drug sensitivities. This condition may be mimicked by U937/CHR2863(200) cells that had 70% residual conversion of CHR2863 to CHR6768 compared to parental U937/WT cells, but acquired a low level of CHR2863 resistance due to reactivation of Akt/mTOR. Akt/mTOR activation in combination with impaired CHR2863 prodrug conversion elicited a high level of resistance in U937/CHR2863(5μM) cells. It is intriguing to note that these phenotypes could be efficiently monitored by assessment of sensitivity to the mTOR inhibitor rapamycin.[53,54] Whereas U937/WT cells, were relatively insensitive to rapamycin, U937/CHR2863(200) cells already gained a substantial increase in rapamycin-sensitivity, which reached a dramatic level of > 1,000-fold increased sensitivity to U937/CHR2863(5μM) cells; this novel finding has major implications for the overcoming of CHR2863 resistance in the clinical setting.[55] Collectively, a multifactorial mechanism appears to underlie acquired resistance to CHR2863 that includes loss of CES1 expression, lack of prodrug conversion as well as mTOR activation.

It is a recurrent theme whether mechanisms of drug resistance observed in model systems will also be operative in a clinical setting. For myeloid leukemia treatment, CHR2797 (Tosedostat) is not administered as single agent but usually in combination with other chemotherapeutics, i.e. daunorubicin and cytarabine, for which CHR2863-resistant U937 myeloid cells retained activity (Table 1).[14] Interestingly, the current study raised some additional potential combinations that may merit further exploration. One would be a combination of CHR2863 with CPT-11/irinotecan which showed collateral sensitivity in CHR2863-resistant U937 cells (Table 1). This is likely attributable to the increased expression of CES2 which facilitates activation of CPT-11.[27,28,56,57] This combination may not only be effective in CHR2863-resistant myeloid cells, but to previously unexposed

cells as CES2 upregulation was also noted after short term CHR2863 exposure (Suppl. Fig. 2A/B). Notably, the role of CES2 in collateral sensitivity to CPT-11 in CHR2863-resistant cells was confirmed by the fact that pharmacologic inhibitors of CES2, e.g. loperamide and benzil abrogated this sensitizing effect (not shown).[58] The opposite response in CES1 and CES2 expression upon CHR2863 exposure may neutralize a potential combination effects for capecitabine as this 5-FU prodrug can be activated by both esterases.[59,60] Lastly, the dramatic gain of sensitivity to rapamycin in U937/CHR2863 cells would call for further examination of combinations of aminopeptidase inhibitor (pro)drugs and rapamycin or other rapalogs. As such, the expanded knowledge of mechanisms underlying loss of efficacy to aminopeptidase inhibitors may guide more rationalized applications of this type of drugs as single agent or in combination therapies, in order to achieve improved therapeutic targeting of monocytes/macrophages in either a cancer or (chronic) inflammatory disease setting.

Acknowledgements

Jorn Smit, Arjo Rutten and Jan Fritz are acknowledged for their skillful technical assistance.This study was supported by CCA-VICI grants 07/36 and 2012-1-08. YG Assaraf is recipient of visiting professor fellowships from the Royal Netherlands Academy of Arts and Sciences, Netherlands Organization for Scientific Research and Cancer Center Amsterdam/VU Institute for Cancer and Immunology.

References

1 Taylor A. Aminopeptidases: structure and function. FASEB J 1993;7:290–8.
2 Saric T, Graef CI, Goldberg AL. Pathway for degradation of peptides generated by proteasomes: a key role for thimet oligopeptidase and other metallopeptidases. J Biol Chem 2004;279:46723–32.
3 Mina-Osorio P. The moonlighting enzyme CD13: old and new functions to target. Trends Mol Med 2008;14:361–71.
4 Santos AN, Langner J, Herrmann M, et al. Aminopeptidase N/CD13 is directly linked to signal transduction pathways in monocytes. Cell Immunol 2000;201:22–32.
5 Sato Y. Role of aminopeptidase in angiogenesis. Biol Pharm Bull 2004;27:772–6.
6 Cifaldi L, Romania P, Lorenzi S, et al. Role of endoplasmic reticulum aminopeptidases in health and disease: from infection to cancer. Int J Mol Sci 2012;13:8338–52.
7 Wickström M, Larsson R, Nygren P, et al. Aminopeptidase N (CD13) as a target for cancer chemotherapy. Cancer Sci 2011;102:501–8.
8 Shimizu T, Tani K, Hase K, et al. CD13/aminopeptidase N-induced lymphocyte involvement in inflamed joints of patients with rheumatoid arthritis. Arthritis Rheum 2002;46:2330–8.
9 Haroon N, Tsui FW, Uchanska-Ziegler B, et al. Endoplasmic reticulum aminopeptidase 1 (ERAP1) exhibits functionally significant interaction with HLA-B27 and relates to subtype specificity in ankylosing spondylitis. Ann Rheum Dis 2012;71:589–95.
10 Lkhagvaa B, Tani K, Sato K, et al. Bestatin, an inhibitor for aminopeptidases, modulates the production of cytokines and chemokines by activated monocytes and macrophages. Cytokine 2008;44:386–91.
11 Ichinose Y, Genka K, Koike T, et al. Randomized double-blind placebo-controlled trial of bestatin in patients with resected stage I squamous-cell lung carcinoma. J Natl Cancer Inst 2003;95:605–10.
12 Ota K, Uzuka Y. Clinical trials of bestatin for leukemia and solid tumors. Biotherapy 1992;4:205–14.
13 Krige D, Needham LA, Bawden LJ, et al. CHR-2797 : An antiproliferative aminopeptidase inhibitor that leads to amino acid deprivation in human leukemic cells. Cancer Res 2008;68:6669–79.
14 Löwenberg B, Morgan G, Ossenkoppele G, et al. Phase I/II clinical study of Tosedostat, an inhibitor of aminopeptidases, in patients with acute myeloid leukemia and myelodysplasia. J Clin Oncol 2010;28:4333–8.
15 Jenkins C, Hewamana S, Krige D, et al. Aminopeptidase inhibition by the novel agent CHR-2797 (tosedostat) for the therapy of acute myeloid leukemia. Leuk Res 2011;35:677–81.
16 Moore HE, Davenport EL, Smith EM, et al. Aminopeptidase inhibition as a targeted treatment strategy in myeloma. Mol Cancer Ther 2009;8:762–70.
17 Reid AHM, Protheroe A, Attard G, et al. A first-in-man phase i and pharmacokinetic study on CHR-2797 (Tosedostat), an inhibitor of M1 aminopeptidases, in patients with advanced solid tumors. Clin Cancer Res 2009;15:4978–85.
18 Van Herpen CML, Eskens F a LM, de Jonge M, et al. A Phase Ib dose-escalation study to evaluate safety and tolerability of the addition of the aminopeptidase inhibitor tosedostat (CHR-2797) to paclitaxel in patients with advanced solid tumours. Br J Cancer 2010;103:1362–8.
19 Needham LA, Davidson AH, Bawden LJ, et al. Drug targeting to monocytes and macrophages using esterase-sensitive chemical motifs. J Pharmacol Exp Ther 2011;339:132–42.
20 Metzeler KH, Hummel M, Bloomfield CD, et al. An 86-probe-set gene-expression signature predicts survival in cytogenetically normal acute myeloid leukemia. Blood 2008;112:4193–201.

21 Scott L, Lamb J, Smith S, et al. Single amino acid (arginine) deprivation: rapid and selective death of cultured transformed and malignant cells. Br J Cancer 2000;83:800–10.
22 Scheffer GL, Kool M, Heijn M, et al. Specific detection of multidrug resistance proteins MRP1, MRP2, MRP3, MRP5, and MDR3 P-glycoprotein with a panel of monoclonal antibodies. Cancer Res 2000;60:5269–77.
23 Verbrugge SE, Assaraf YG, Dijkmans BAC, et al. Inactivating PSMB5 mutations and P-glycoprotein (multidrug resistance-associated protein/ATP-binding cassette B1) mediate resistance to proteasome inhibitors: ex vivo efficacy of (immuno)proteasome inhibitors in mononuclear blood cells from patients with . J Pharmacol Exp Ther 2012;341:174–82.
24 Li HY, Appelbaum FR, Willman CL, et al. Cholesterol-modulating agents kill acute myeloid leukemia cells and sensitize them to therapeutics by blocking adaptive cholesterol responses. Blood 2003;101:3628–34.
25 Van de Ven R, Oerlemans R, van der Heijden JW, et al. ABC drug transporters and immunity: novel therapeutic targets in autoimmunity and cancer. J Leukoc Biol 2009;86:1075–87.
26 Redinbo MR, Potter PM. Mammalian carboxylesterases: from drug targets to protein therapeutics. Drug Discov Today 2005;10:313–25.
27 Sanghani SP, Sanghani PC, Schiel MA, et al. Human carboxylesterases: an update on CES1, CES2 and CES3. Protein Pept Lett 2009;16:1207–14.
28 Imai T, Taketani M, Shii M, et al. Substrate specificity of carboxylesterase isozymes and their contribution to hydrolase activity in human liver and small intestine. Drug Metab Dispos 2006;34:1734–41.
29 Ghosh S, Zhao B, Bie J, et al. Macrophage cholesteryl ester mobilization and atherosclerosis. Vasc Pharmacol 2010;52:1–10.
30 Crow JA, Middleton BL, Borazjani A, et al. Inhibition of carboxylesterase 1 is associated with cholesteryl ester retention in human THP-1 monocyte/macrophages. Biochim Biophys Acta 2008;1781:643–54.
31 Blais DR, Lyn RK, Joyce MA, et al. Activity-based protein profiling identifies a host enzyme, carboxylesterase 1, which is differentially active during hepatitis C virus replication. J Biol Chem 2010;285:25602–12.
32 Welte MA. Proteins under new management: lipid droplets deliver. Trends Cell Biol 2007;17:363–9.
33 Wan HC, Melo RC, Jin Z, et al. Roles and origins of leukocyte lipid bodies: proteomic and ultrastructural studies. FASEB J 2007;21:167–78.
34 Bozza PT, Magalhães KG, Weller PF. Leukocyte lipid bodies - Biogenesis and functions in inflammation. Biochim Biophys Acta 2009;1791:540–51.
35 Zoncu R, Efeyan A, Sabatini DM. mTOR: from growth signal integration to cancer, diabetes and ageing. Nat Rev Mol Cell Biol 2011;12:21–35.
36 Gonen N, Assaraf YG. Antifolates in cancer therapy: structure, activity and mechanisms of drug resistance. Drug Resist Updat 2012;15:183–210.
37 Oerlemans R, Franke NE, Assaraf YG, et al. Molecular basis of bortezomib resistance: proteasome subunit beta5 (PSMB5) gene mutation and overexpression of PSMB5 protein. Blood 2008;112:2489–99.
38 Adar Y, Stark M, Bram EE, et al. Imidazoacridinone-dependent lysosomal photodestruction: a pharmacological Trojan horse approach to eradicate multidrug-resistant cancers. Cell Death Dis 2012;3:293–9.
39 Zhao B, Fisher BJ, St Clair RW, et al. Redistribution of macrophage cholesteryl ester hydrolase from cytoplasm to lipid droplets upon lipid loading. J Lipid Res 2005;46:2114–21.
40 Zhao B, Song J, St Clair RW, et al. Stable overexpression of human macrophage cholesteryl ester hydrolase results in enhanced free cholesterol efflux from human THP1 macrophages. Am J Physiol Cell Physiol 2007;292:405–12.

41 Zhao B, Bie J, Wang J, et al. Identification of a novel intracellular cholesteryl ester hydrolase (carboxylesterase 3) in human macrophages: compensatory increase in its expression after carboxylesterase 1 silencing. Am J Physiol Cell Physiol 2012;303:427–35.
42 Pu J, Ha CW, Zhang S, et al. Interactomic study on interaction between lipid droplets and mitochondria. Protein Cell 2011;2:487–96.
43 Skinner-Adams TS, Peatey CL, Anderson K, et al. The aminopeptidase inhibitor CHR-2863 is an orally bioavailable inhibitor of murine malaria. Antimicrob Agents Chemother 2012;56:3244–9.
44 Coppens I, Vielemeyer O. Insights into unique physiological features of neutral lipids in Apicomplexa: from storage to potential mediation in parasite metabolic activities. Int J Parasitol 2005;35:597–615.
45 Pisciotta JM, Coppens I, Tripathi AK, et al. Insights into unique physiological features of neutral lipids in Apicomplexa: from storage to potential mediation in parasite metabolic activities. Biochem J 2007;402:197–204.
46 Rius M, Hummel-Eisenbeiss J, Keppler D. ATP-dependent transport of leukotrienes B4 and C4 by the multidrug resistance protein ABCC4 (MRP4). J Pharmacol Exp Ther 2008;324:86–94.
47 Bozza PT, Bakker-Abreu I, Navarro-Xavier RA, et al. Lipid body function in eicosanoid synthesis: an update. Prostaglandins Leukot Essent Fat Acids 2011;85:205–13.
48 Reid G, Wielinga P, Zelcer N, et al. The human multidrug resistance protein MRP4 functions as a prostaglandin efflux transporter and is inhibited by nonsteroidal antiinflammatory drugs. Proc Natl Acad Sci U S A 2003;100:9244–9.
49 Goodman JM. The gregarious lipid droplet. J Biol Chem 2008;283:28005–9.
50 Farese RVJ, Walther TC. Lipid droplets finally get a little R-E-S-P-E-C-T. Cell 2009;139:855–60.
51 Greenberg AS, Coleman RA, Kraemer FB, et al. The role of lipid droplets in metabolic disease in rodents and humans. J Clin Invest 2011;121:2102–10.
52 Avruch J, Long X, Ortiz-Vega S, et al. Amino acid regulation of TOR complex 1. Am J Physiol Endocrinol Metab 2009;296:E592–602.
53 Laplante M, Sabatini DM. mTOR signaling in growth control and disease. Cell 2012;149:274–93.
54 Chapuis N, Tamburini J, Green AS, et al. Perspectives on inhibiting mTOR as a future treatment strategy for hematological malignancies. Leukemia 2010;24:1686–99.
55 Böhm A, Aichberger KJ, Mayerhofer M, et al. Targeting of mTOR is associated with decreased growth and decreased VEGF expression in acute myeloid leukaemia cells. Eur J Clin Invest 2009;39:395–405.
56 Humerickhouse R, Lohrbach K, Li L, et al. Characterization of CPT-11 hydrolysis by human liver carboxylesterase isoforms hCE-1 and hCE-2. Cancer Res 2000;60:1189–92.
57 Satoh T, Hosokawa M. Structure, function and regulation of carboxylesterases. Chem Biol Interact 2006;162:195–211.
58 Fukami T, Takahashi S, Nakagawa N, et al. In vitro evaluation of inhibitory effects of antidiabetic and antihyperlipidemic drugs on human carboxylesterase activities. Drug Metab Dispos 2010;38:2173–8.
59 Quinney SK, Sanghani SP, Davis WI, et al. Hydrolysis of capecitabine to 5'-deoxy-5-fluorocytidine by human carboxylesterases and inhibition by loperamide. J Pharmacol Exp Ther 2005;313:1011–6.
60 Guichard SM, Macpherson JS, Mayer I, et al. Gene expression predicts differential capecitabine metabolism, impacting on both pharmacokinetics and antitumour activity. Eur J Cancer 2008;44:310–7.

SUPPLEMENTAL MATERIAL

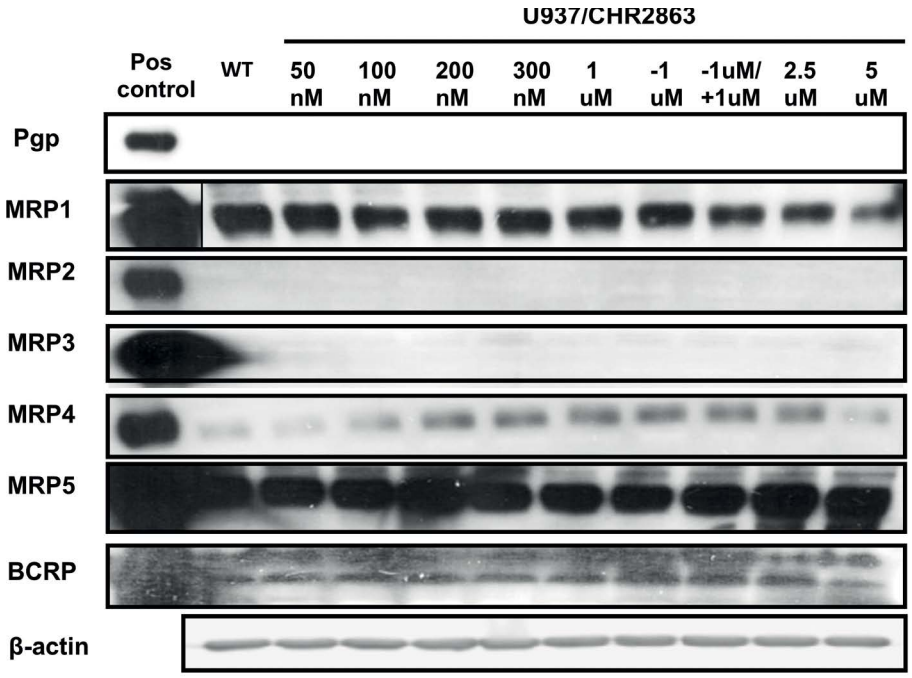

Figure S1: *Expression levels of various established drug efflux transporters of the ATP-Binding Cassette family in U937/WT cells and U937 cells selected for growth in the presence of 50 nM to 5μM CHR2863. U937/CHR2863(-1 μM) refers to U937/CHR2863(1 μM) grown without CHR2863 for 2 weeks, whereas U937/CHR2863(-1μM/+1μM) after rechallenge with 1 μM CHR2863 for 2 weeks. Positive controls included previously reported cell lines overexpressing each of these transporters.*[22,23]

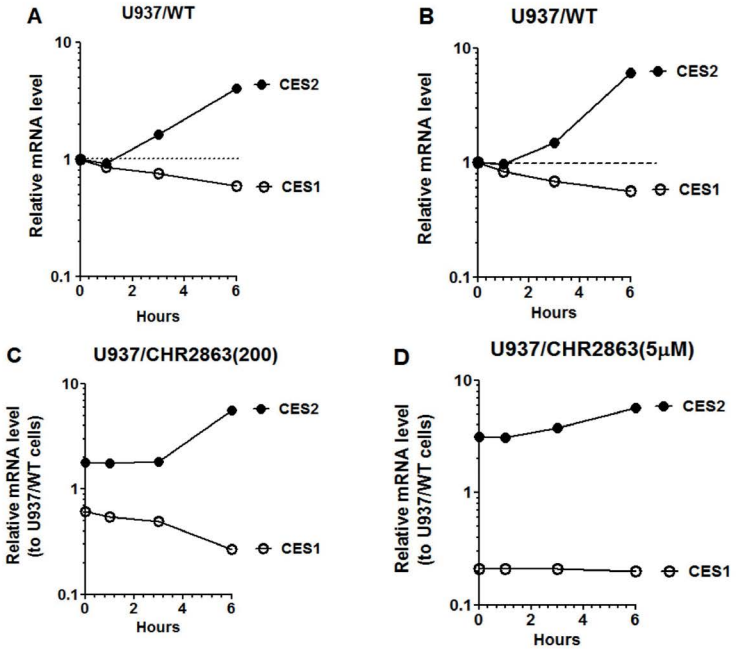

Figure S2: *Dynamics of CES1 and CES2 mRNA expression following 0-6 hours exposure of (A) U937/WT cells + 50 nM CHR2863, (B) U937/WT + 6 μM CHR2863, (C) U937/CHR2863(200) + 6 μM CHR2863, and (D) U937/CHR2863(5μM) cells + 6 μM CHR2863. Results are expressed relative to values of U937/WT at t=0, and depict the mean of two experiments performed in triplicate.*

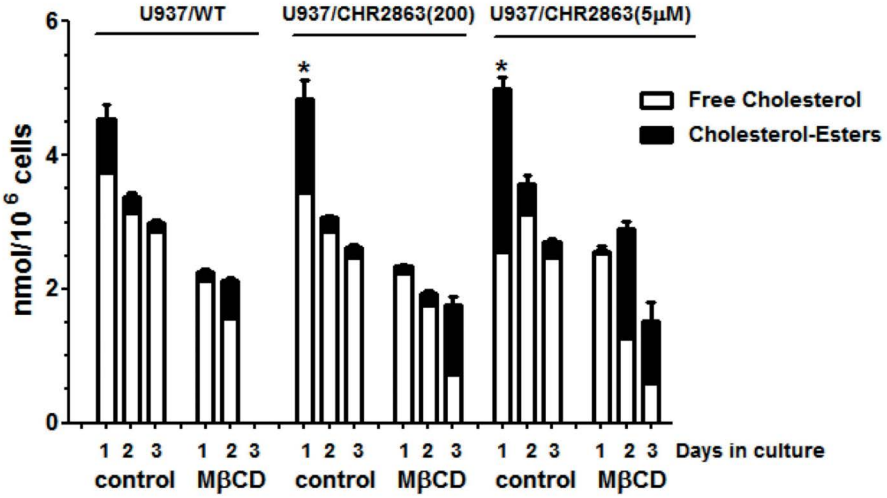

Figure S3: *Free cholesterol and cholesteryl ester content in U937/WT, U937/CHR2863(200), and U937/CHR2863(5μM) cells during 3 days cell culture, with, for the CHR2863-resistant cells, in the presence of their selective concentrations of CHR2863. As a control experiments were performed in the presence of 1 mM of cholesterol-lowering drug methyl-β-cyclodextrin (MβCD). Results are the mean ± SD of 3 separate experiments performed in duplicate.*